Desalination and Water Treatment
www.deswater.com

doi: 10.1080/19443994.2016.1144762

57 (2016) 23246–23256
October

Taylor & Francis
Taylor & Francis Group

The effect of feed pretreatment on membrane microfiltration of titanium dioxide dispersions by ceramic tubular membranes

Miroslav Grulich*, Petr Mikulášek

Faculty of Chemical Technology, Institute of Environmental and Chemical Engineering, University of Pardubice, Studentská 573, 532 10 Pardubice, Czech Republic, Tel. +420 466037350; email: Miroslav.Grulich@upce.cz (M. Grulich), Tel. +420 466 037 503; email: Petr.Mikulasek@upce.cz (P. Mikulášek)

Received 27 March 2015; Accepted 10 January 2016

ABSTRACT

The influence of coagulant type and operating parameters on crossflow microfiltration of aqueous dispersions of titanium dioxide has been examined. The experiments were carried out with a tubular ceramic microfiltration membrane with a nominal pore size of 0.1 μm at various operating parameters. Three chosen types of organic coagulants were used for a series of crossflow microfiltration experiments: polyacrylamide (PAM), poly(diallyldimethylammonium chloride) (PDADMAC), and poly(acrylamide-co-acrylic acid) partial sodium salt (PACA). The value of steady-state permeate flux has been experimentally evaluated for the crossflow microfiltration with and without pretreatment. The results of the experiments without coagulants showed that the flux initially declines rapidly and then stabilizes. The results also suggested that PDADMAC was a better coagulant for this system and its optimal concentration was 30 mg l^{-1}. Finally, it was shown that pretreatment of the feed by PDADMAC resulted in a permeate flux that was more than three times higher than that obtained without any pretreatment. Moreover, there was a very positive effect of this coagulant on the particle size. Pretreatment by 30 mg l^{-1} PDADMAC led to an average particle size that was almost 18 times higher than that obtained without pretreatment. The other two coagulants did not produce such improvements: pretreatment of the feed by PAM increased the permeate flux by only 10%, while pretreatment by PACA gave even lower permeate flux than no pretreatment. This means that the results of various experiments have shown the need for careful selection of the coagulant due to their differing influences on the permeate flux. The relationship between the particle size of the dispersion and the permeate flux was found from the results of these experiments. A published mathematical model was used to estimate the permeate flux. The results of the experiments showed that the mathematical model was able to predict the steady-state permeate flux quite accurately in some cases.

Keywords: Microfiltration; Coagulation; Particle size; Titanium dioxide; Ceramic membrane

*Corresponding author.

Presented at EuroMed 2015: Desalination for Clean Water and Energy Palermo, Italy, 10–14 May 2015. Organized by the European Desalination Society.

1944-3994/1944-3986 © 2016 Balaban Desalination Publications. All rights reserved.

1. Introduction

Membrane microfiltration is a pressure-driven process with a microporous membrane as the separating medium [1]. The pore sizes of microfiltration membranes range from 10 to 0.05 μm, making the process suitable for retaining suspensions and emulsions. Microfiltration is the membrane process which most closely resembles conventional coarse filtration [2].

Basically, microfiltration can be operated in two modes: (i) dead-end and (ii) crossflow. In a dead-end arrangement, the entire feed flow is transported toward the membrane perpendicularly so that the retained particles and other components are accumulated and deposited onto the membrane surface. As opposed to dead-end microfiltration, in a crossflow operation, the feed stream moves parallel to the membrane surface and only a portion of the feed stream passes through the membrane under the driving pressure [3]. The tangential flow generates the respective forces that tend to remove the deposited layers from the membrane surface, helping to keep it relatively clean. The operational cost of the crossflow mode is higher than that of the dead-end mode because of the energy needed to circulate the feed. The circulation of the dispersion around the membrane surface and the permeate removal result in increasing concentrations of a component in the retentate and in the decreasing flux, respectively [4].

When microfiltration is applied using constant pressure filtration, the main problem encountered is the flux decline, while if microfiltration is applied using constant flux filtration, the main problem is the increase in pressure loss. This is caused by the concentration polarization and fouling, the latter being the deposition of solutes at the membrane surface or inside the pores of the membrane (plugging). The steady-state permeate flux may be as low as 2–10% of pure water flux [2].

The flux decline can be reduced using two groups of special methods. The first group requires a discontinuation process, namely chemical and mechanical cleaning or backwashing. The second group of methods can be used without discontinuation (e.g. feed pretreatment, influencing the interaction phenomena between the particles and the surface of the membrane, hydrodynamic methods) [5]. One of the suitable feed pretreatment methods is coagulation, for which the respective coagulants can be divided into several categories such as simple inorganic coagulants, prehydrolyzed metal salts, organic polymers, and natural coagulants. The selection of these chemicals and flocculation aids for use in a particular plant is generally based on economic considerations along with reliability, safety, and chemical storage considerations. The best methods of determining the treatability, the most effective coagulants, and the required dosages are to conduct jar tests, bench-scale tests, and in some cases, pilot tests [6].

Microfiltration is used in a wide variety of industrial applications. The most important applications of microfiltration are wastewater treatment, sterilization, clarification of all kinds of beverages and pharmaceuticals in the food and pharmaceutical industries, and removal of particles during the processing of ultrapure water in the semiconductor industry [7].

In the literature, we were able to find many studies of feed pretreatment. Erdei et al. [8] and Park et al. [9] investigated coagulation and its effect on the flux decline and the removal of pollutants in wastewater treatment. The results of these studies show that coagulation has a positive effect on the flux decline and on the removal of colloidal pollutants from wastewater. Erdei et al. [8] also found that the results are highly dependent on the type of coagulant. Zhu et al. [10] reported on membrane fouling in wastewater treatment; the results obtained showed that coagulant dosage had a clear influence on membrane fouling during microfiltration. Furthermore, Bhattacharya et al. [11] investigated the microfiltration of textile industry water with pretreatment by coagulation with ceramic membrane. Their results revealed that the optimal coagulant dosage gave a dye removal rate of about 96%, while a higher dosage of coagulant achieved only about 85% removal.

Zhao et al. [12] and Wang et al. [13] investigated the effect of coagulation on the formation of particles and particle size. Their studies showed that coagulation had positive effects on the particle size and permeate flux. The proper choice of the type of coagulant had a significant effect on the structure and size of the particles. In contrast, Hofs et al. [14] found that coagulation could have a negative effect on membrane fouling. In their study, coagulation had a positive effect on reversible membrane fouling but a negative effect on irreversible membrane fouling.

Finally, Wang et al. [15] studied the factors and mechanisms of fouling of microfiltration membranes by organic polymers which had been used for the feed pretreatment. The obtained results confirmed that high concentrations of coagulant could cause clogging of the membrane due to the presence of free polymer molecules. Wu et al. [16] outlined similar conclusions, ascertaining that use of the optimal coagulant concentration reduced the risk of membrane fouling, whereas a higher concentration led to membrane fouling due to blocking of the membrane pores by the added coagulants.

1.1. Model development

This semi-empirical mathematical model [17] aims to build the relationship between steady-state permeate flux and the particle size of the dispersion, which may be helpful for understanding membrane microfiltration performance.

The volume flow through the membrane can be described by Darcy's law, with the flux through the membrane being directly proportional to the applied transmembrane pressure:

$$J = K\Delta P \tag{1}$$

where K is the membrane permeability and ΔP is the pressure difference.

According to the resistance in series model, Darcy's law was changed to the form in which the permeate flux is expressed as a ratio of the transmembrane pressure to the permeate flow resistance:

$$J = \frac{\Delta P}{\mu_0 R_t} \tag{2}$$

where μ_0 is the dynamic viscosity of solvent and R_t is the total resistance to permeate flow.

The resistance in series model assumes that several additive resistances affect permeate flux:

$$R_t = R_c + R_m + R_f \tag{3}$$

where R_c is the resistance of the filtration cake, R_m is the resistance of the membrane, and R_f is the resistance caused by blocking of pores and adsorption on their surface.

The resistance of the filtration cake can be expressed as a function of the cake resistance per unit thickness ($\hat{R}_c$):

$$R_c = \hat{R}_c\,\delta_c \tag{4}$$

where δ_c is the thickness of the filtration cake.

By combining Eqs. (3) and (4), Eq. (2) can be rewritten in the form:

$$J = \frac{\Delta P}{\mu_0\left[\left(\hat{R}_c\,\delta_c\right) + R_m + R_f\right]} \tag{5}$$

For negligible membrane resistance and the resistance caused by pores blocking compared to the resistance of a filtration cake, Eq. (5) may be expressed as:

$$J = \frac{\Delta P}{\mu_0\left(\hat{R}_c\,\delta_c\right)} \tag{6}$$

It is important to establish the mass balance of microfiltration (mass balance in dead-end microfiltration), which can be expressed as:

$$\left(J + \frac{d\delta_c}{dt}\right)\Phi_b = \Phi_c\frac{d\delta_c}{dt} \tag{7}$$

where Φ_b is the particle volume fraction of the dispersion and Φ_c is the particle volume fraction in the filtration cake. The left side of Eq. (7) describes the flux of particles into the surface of the cake, while the right side of Eq. (7) describes the buildup of particles in the cake.

In crossflow microfiltration, the effect of turbulence on the filtration cake is defined as:

$$k_1\left(\frac{dU}{dy}\right)\delta_c \tag{8}$$

where k_1 is the particle constant and dU/dy is the velocity gradient where dU is the flow velocity difference between the layers and dy is the distance between the layers.

The new term representing the particle mass balance that reflects the effect of turbulence can be obtained from Eqs. (7) and (8):

$$\left(J + \frac{d\delta_c}{dt}\right)\Phi_b - k_1\left(\frac{dU}{dy}\right)\delta_c = \Phi_c\frac{d\delta_c}{dt} \tag{9}$$

By combining Eqs. (6) and (9), the following can be obtained:

$$\frac{d\delta_c}{dt} = \frac{\Delta P\Phi_b}{\mu_0\,\hat{R}_c\,\delta_c(\Phi_c - \Phi_b)} - \frac{k_1(dU/dy)\delta_c}{\Phi_c - \Phi_b} \tag{10}$$

Assuming zero thickness of the filtration cake at the start of separation, constant transmembrane pressure during microfiltration, a constant shear rate, and specific resistance of the filtration cake, Eq. (10) can be integrated:

$$\delta_c(t) = \sqrt{\frac{\Delta P\Phi_b}{\hat{R}_c\,k_1\mu_0\left(\frac{dU}{dy}\right)}\left(1 - \exp\left(-\frac{2k_1\left(\frac{dU}{dy}\right)t}{\Phi_c - \Phi_b}\right)\right)} \tag{11}$$

By combining Eqs. (5) and (11), a generic term describing the permeate flow in time can be obtained:

$$J(t) = \frac{\Delta P}{\left[\sqrt{\frac{\Delta P\,\Phi_b\,\mu_0\,\hat{R}_c}{k_1\left(\frac{dU}{dy}\right)}\left(1-\exp\left(-\frac{2k_1\left(\frac{dU}{dy}\right)t}{\Phi_c-\Phi_b}\right)\right)}\right] + \mu_0(R_m + R_f)} \tag{12}$$

For Newtonian fluids, the velocity gradient may be replaced by the expression:

$$\frac{dU}{dy} = \frac{\tau_w}{\mu} \tag{13}$$

where τ_w is the shear stress at the membrane wall and μ is the dynamic viscosity of a suspension.

By combining Eqs. (12) and (13), the following can be obtained:

$$J(t) = \frac{\Delta P}{\left[\sqrt{\frac{\Delta P\,\Phi_b\,\mu_0\,\mu\,\hat{R}_c}{k_1\tau_w}\left(1-\exp\left(-\frac{2k_1\,\tau_w\,t}{\mu(\Phi_c-\Phi_b)}\right)\right)}\right] + \mu_0(R_m + R_f)} \tag{14}$$

However, a number of substances form a compressible filtration cake. Porter [18] suggests a relationship to estimate the influence of the compressibility of the filter cake on the cake resistance per unit thickness in the form:

$$\hat{R}_c = \alpha_0(\Delta P)^s\rho_s\Phi_c \tag{15}$$

where α_0 is the particle constant, s is the filtration cake compressibility constant, and ρ_s is the density of the particles constituting the filtration cake.

By combining Eqs. (14) and (15), the following can be obtained:

$$J(t) = \frac{\Delta P}{\left[\sqrt{\frac{\Delta P^{(1+s)}\Phi_b\,\mu_0\,\mu\,\alpha_0\,\rho_s\,\Phi_c}{k_1\,\tau_w}\left(1-\exp\left(-\frac{2k_1\,\tau_w\,t}{\mu(\Phi_c-\Phi_b)}\right)\right)}\right] + \mu_0(R_m + R_f)} \tag{16}$$

Then, for the steady-state permeate flux,

$$\lim_{t\to\infty}\exp\left(-\frac{2k_1\,\tau_w\,t}{\mu(\Phi_c-\Phi_b)}\right) = 0 \tag{17}$$

For an incompressible filtration cake and negligible resistance by blocking of pores, the resulting equation for the steady-state permeate flux can be written in the form:

$$J(t) = \frac{\Delta P}{\sqrt{\frac{\Delta P\,\Phi_b\,\mu_0\,\mu\,\alpha\,\rho_s\,\Phi_c}{\tau_w}} + \mu_0\,R_m} \tag{18}$$

2. Experimental

The microfiltration experiments were carried out with an aqueous dispersion of titanium dioxide (anatase form; PRECHEZA, Czech Republic). Dispersions were prepared from powdered titanium dioxide and deionized water at a concentration of 3 wt.% TiO_2.

Titanium dioxide was chosen for the experiments because of the continuity to previous works at our research institute. Other reasons include the polydispersity of powdered titanium dioxide, which predestines it as a suitable dispersion model with realistic properties. Finally, an important argument for this choice is the practical use of dispersions of titanium dioxide, especially in its production and in many other practical applications, since titanium dioxide is used in many applications, for example, as an additive to foods, pharmaceuticals, and paints.

Fig. 1 shows the particle size distribution of the dispersion without pretreatment. The average particle size of the dispersion was 0.486 μm, while the particle size distribution curve showed two maxima. The first one was the major peak, with an average particle size of about 0.5 μm, whereas the second peak had an average particle size of about 10 μm.

The particle size distributions were measured by a Mastersizer 2000 MU instrument (Malvern Instruments, UK) and by a Zetasizer Nano ZS (Malvern Instruments, UK). By employing the Mastersizer 2000 MU, the particle size measurements were performed using laser diffraction and the measured particle size ranged from 0.02 to 2,000 μm. The Zetasizer Nano ZS was then used to perform the particle size measurements with the aid of a process called dynamic light

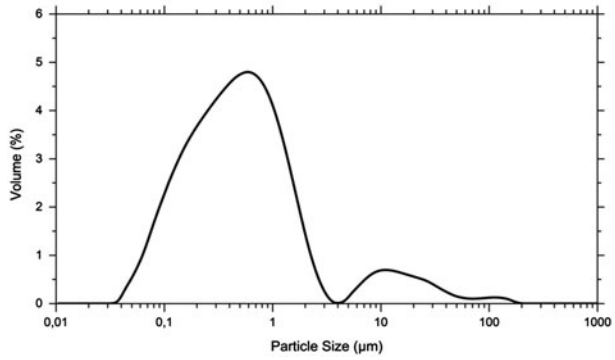

Fig. 1. Particle size distribution of the titanium dioxide dispersion used (measured by a Mastersizer 2,000 MU).

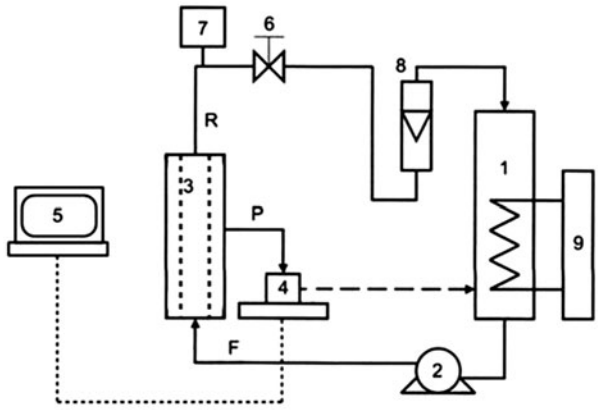

Fig. 2. Schematic diagram of the experimental equipment. Notes: (1) Storage tank, (2) pump, (3) membrane module, (4) electronic balance, (5) PC, (6) regulating valve, (7) manometer, (8) flowmeter, (9) thermoregulator, (F) feed, (P) permeate, (R) retentate.

scattering (DLS). In this case, the device measured the Brownian motion of particles, displaying it in relation to their size. The particle size of the Zetasizer Nano ZS was measured in the range from 0.6 to 6 μm.

In the separation experiments, asymmetric α-Al_2O_3 microfiltration membranes (Terronic, Czech Republic) were used. They were configured as single cylindrical tubes, 25-cm long, 6 mm in inner diameter, and 10 mm in outer diameter, with the active layer deposited on the internal surface of the tubular support. The basic properties of the membrane are shown in Table 1.

Microfiltration was operated in the crossflow configuration and the corresponding experimental equipment is shown in Fig. 2. The feed dispersion was pumped from the storage tank (1) to the membrane module (3) by a positive displacement diaphragm pump (2) (Hydra-Cell Pump) with a frequency converter to control the speed (model VA 02B-03, TOS Kuřim; Czech Republic). The permeate flux was measured by an electronic balance (4) (model KERN 573–46NM, Kern, Germany) connected to a personal computer (5) via an RS 232 serial communication port. The retentate was returned to the storage tank, and the permeate was also returned to the feed tank to maintain a constant feed concentration. The pressure was adjusted to the target value by a regulating valve (6) and the overpressure was measured by a manometer (7) (model TMG 567 C3H, Cressto, Czech Republic). The flow rate of the feed was determined by a flowmeter (8) and the temperature of the feed was kept constant by the thermoregulation system (9).

Table 1
Membrane characteristics

Producer	Terronic
Material	α-Al_2O_3
Geometry	Tubular
Nominal pore diameter	0.1 μm
Membrane area	43.35 cm^2
Permeability	1,894.9 l m^{-2} h^{-1} bar^{-1}

Three types of organic coagulants were used for the crossflow microfiltration experiments: (i) polyacrylamide (PAM) 50 wt.% solution, (ii) poly(diallyldimethylammonium chloride) (PDADMAC) 20 wt.% solution, and (iii) poly(acrylamide-co-acrylic acid) partial sodium salt (PACA) 80 wt.% solution. All three coagulants were purchased from Sigma–Aldrich. The formulas of the coagulants are shown in Table 2.

Different coagulation abilities of tested coagulants may be caused by different mechanisms of coagulation. The tested coagulant PDADMAC is a cationic polymer with medium average molecular weight and a high charge density. High charged polymers tend to produce flocs with higher particle size and therefore induce electrostatic patch flocculation [19]. According to Blanco et al. [20], PDADMAC produces flocs by charge neutralization. In contrast, PAM is a polymer with low average molecular weight and low charge density producing flocs by bridging [20].

For each experiment, coagulant was added to the dispersion, which was then homogenized by stirring at 2,000 rpm for 30 s and then at 100 rmp for 20 min. Next, the dispersion was poured into the experimental equipment. The same procedure was performed to measure the particle size of the dispersion.

During all the tests, the microfiltration process was run at a constant crossflow velocity of 2 m s^{-1} and a pressure difference of 100 kPa, with the temperature

Table 2
Coagulant characteristics

Coagulant	Average molecular weight (g mol^{-1})	Formula
PAM	10,000	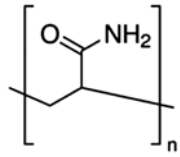
PDADMAC	400,000–500,000	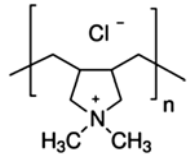
PACA	520,000	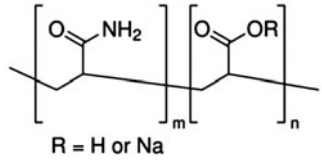

of the dispersion being 20°C. The particle size distributions were determined by a Mastersizer MU 2000 (Malvern Instruments).

3. Results and Discussion

In order to select the optimum dose of coagulant, different doses were tested and their influence on the crossflow microfiltration process with respect to the steady-state values of permeate flux and particle size distribution was studied.

3.1. Pretreatment by PAM

The dependencies of the flux–time curve on PAM dosage are shown in Fig. 3. From this figure, it is evident that the influence of PAM on the steady-state permeate flux is positive. In Fig. 3, we can also see that the optimal dose of PAM among the doses tested is 100 mg l^{-1}. The results with the higher dose (200 mg l^{-1}) are worse than those with the lower one and even worse than for the experiment without pretreatment.

In Fig. 4, we can see the effect of PAM dosage on the particle size distribution. It is evident that the distribution curves for all concentrations of coagulant have a similar character. The results indicate that the dispersion with the highest concentration of coagulant (200 mg l^{-1}) contained smaller particles than the dispersion without pretreatment. This can be explained by the fact that these small particles have a tendency to block (clog) the membrane pores. In Fig. 3, we can

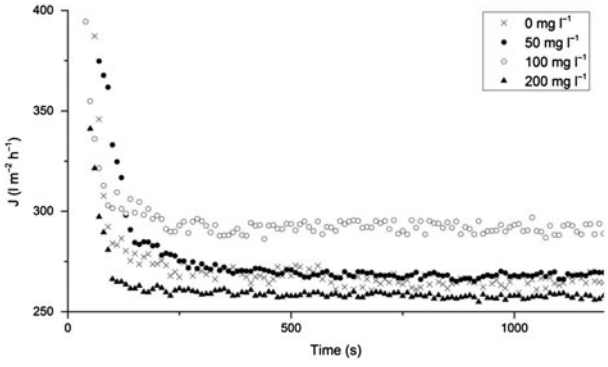

Fig. 3. Effect of PAM dosage on flux–time curve during crossflow microfiltration.

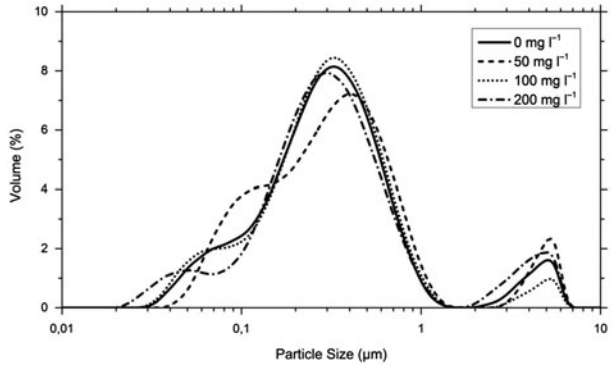

Fig. 4. Effect of PAM dosage on particle size distribution (measured by Zetasizer Nano ZS).

see that the clogging of the membrane pores caused a lower steady-state permeate flux during the membrane separation due to the high concentration of coagulant.

3.2. Pretreatment by PACA

Fig. 5 depicts the dependencies of the flux–time curve on the PACA dosage, revealing that the influence of PACA on the steady-state permeate flux is negative. It can also be seen that the steady-state flux increases as the dosage of coagulant increases.

It can be stated that all the tested concentrations of coagulant gave worse results than the experiment without pretreatment. Thus, the coagulant PACA was not suitable for this system as it reduced the steady-state permeate flux compared to the experiments without pretreatment.

In Fig. 6, we can see the effect of PACA dosage on the particle size distribution. It is evident that the distribution curves for the dispersion prepared using the coagulant had different characteristics compared to the distribution curve of dispersion without pretreatment. Also, the distribution curves for all concentrations of coagulant are similar in the area of the main peak, except in the case with a small particle size, where the respective distribution differs from the distribution curve of dispersion obtained by the same process without pretreatment. Dispersions pretreated by PACA coagulant contained smaller particles than the dispersion without pretreatment, namely, concentrations of 20 and 50 mg l^{-1} led to particles sizes of 20–50 nm. At the highest concentration of the coagulant (100 mg l^{-1}), the dispersion contains particles larger than 10 nm. These trends toward the production of smaller particles when the concentration of PACA coagulant increases demonstrate why the increasing concentration of PACA coagulant gives rise to a decrease in the steady-state permeate flux. This probably occurred because the very small particles were smaller than the membrane pores, which may have caused the above-mentioned clogging. These effects of blocking of membrane pores by small particles then resulted in a lower steady-state permeate flux of the pretreated dispersion compared to the experiment in which the dispersion was not pretreated.

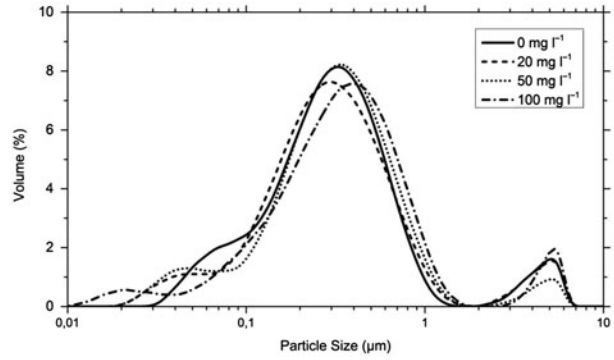

Fig. 6. Effect of PACA dosage on particle size distribution (measured by Zetasizer Nano ZS).

3.3. Pretreatment by PDADMAC

The dependencies of the flux–time curve on PDADMAC dosage are shown in Fig. 7. This figure reveals the benefit of using PDADMAC in comparison with the other two types of coagulants. The figure also reveals that the optimal dose of PDADMAC is 30 mg l^{-1}; nevertheless, the results with higher doses (40 or 50 mg l^{-1}, respectively) are very similar. Otherwise, the results also show that pretreatment of the feed by PDADMAC led to permeate flux that was

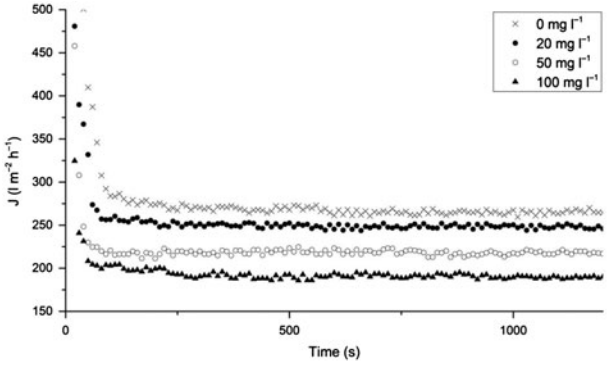

Fig. 5. Effect of PACA dosage on flux–time curve during crossflow microfiltration.

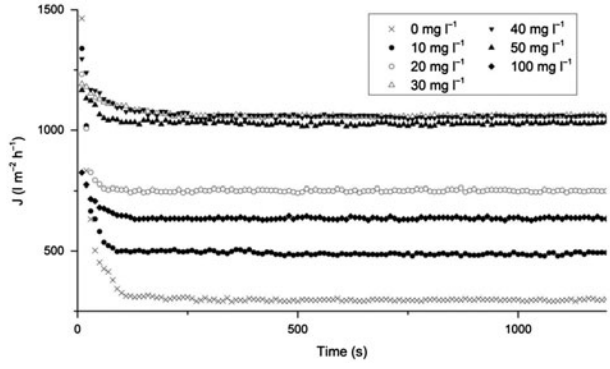

Fig. 7. Effect of PDADMAC dosage on flux–time curve during crossflow microfiltration.

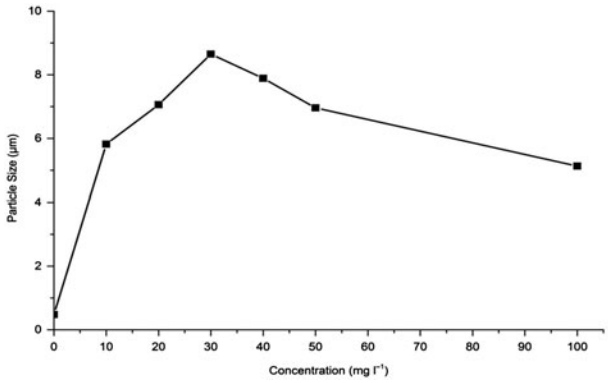

Fig. 8. Effect of PDADMAC dosage on average particle size (measured by Mastersizer MU 2,000).

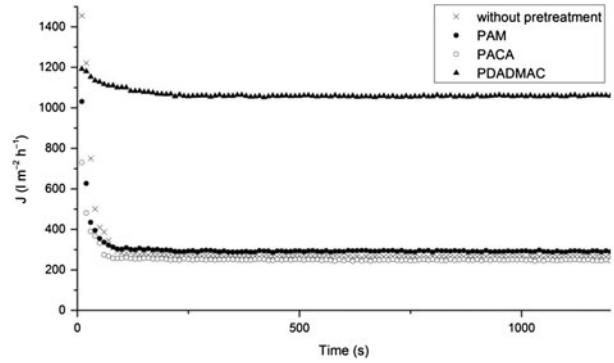

Fig. 9. Effect of coagulant addition at optimum dosage on the flux–time curve during crossflow microfiltration.

more than three times higher than in the conditions without any pretreatment. It can be stated that the application of a higher dose (100 mg l^{-1}) led to worse results than the optimal dose but still gave better performance than the experiments without pretreatment.

Next, we explored the effect of PDADMAC dosage on the average particle size, which is plotted in Fig. 8. As can be seen, the particle sizes are highly variable with different concentrations of coagulant, as even the lowest concentration of coagulant caused an abrupt increase in particle size.

The largest average particle size of the dispersion was obtained at the optimum concentration of coagulant (30 mg l^{-1}). At this concentration, the average particle size was 8.65 μm, which was 18 times higher than the average particle size in the experiments without pretreatment.

At concentrations of coagulant higher than 30 mg l^{-1}, the particle size decreased, confirming the results of the microfiltration tests and the previously observed changes in the steady-state permeate fluxes.

The filtration cake seemed more compact and sticky at high doses of the coagulant than at the optimal dose. This fact and the decrease in the particle size are probably caused by free molecules of the coagulant in the dispersion.

3.4. Comparison of coagulants

In Fig. 9, the dependencies of the flux–time curve for the coagulants tested and their optimal dosages are shown. From this comparison, it is evident that the most suitable coagulant for the system used is PDADMAC at the optimum dosage of 30 mg l^{-1}. The other two coagulants did not produce such an improvement as PDADMAC, because the pretreatment by PAM and PACA led only to insignificant enhancement of the permeate flux. Pretreatment of the feed by PAM resulted in a negligible improvement, that is, a ca. 10% higher permeate flux compared to that obtained without pretreatment, while the application of PACA led to an even lower permeate flux than that obtained without pretreatment. Thus, the experimental results revealed the need for careful selection of the coagulant, because different coagulants had considerably different impacts on the permeate flux.

3.5. Effect of transmembrane pressure on microfiltration (limiting flux)

The dependencies of the flux–time curve on transmembrane pressure during the experiments without pretreatment are compared in Fig. 10. From this figure, it is evident that the permeate flux increases with higher transmembrane pressure but this increase is not linear. For example, when the transmembrane pressure increases from 50 to 100 kPa, the steady-state permeate flux increases from 207.9 to 265 l m^{-2} h^{-1}, which is an increase of 57.1 l m^{-2} h^{-1}, while if the

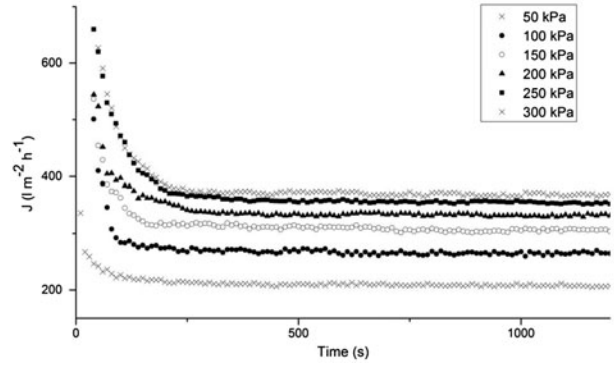

Fig. 10. Effect of pressure difference on flux–time curve during crossflow microfiltration (without pretreatment).

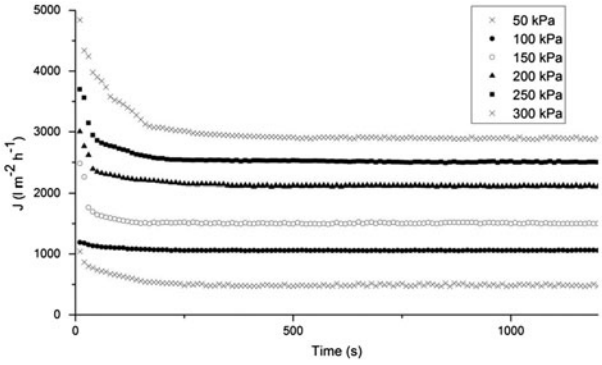

Fig. 11. Effect of pressure difference on flux–time curve during crossflow microfiltration (pretreatment with 30 mg l^{-1} PDADMAC).

transmembrane pressure increases from 250 to 300 kPa the steady-state permeate flux increases from 354.6 to 368.6 l m^{-2} h^{-1}, which is an increase of only 14 l m^{-2} h^{-1}. From these values, it is evident that this system exhibits a limiting flux. The limiting flux represents the maximum stationary permeation flux which can be reached when increasing the transmembrane pressure [21].

Fig. 11 depicts the effect of the transmembrane pressure on the flux–time curve during experiments with pretreatment using 30 mg l^{-1} PDADMAC. Under the same pressure differences as in the case of dispersion without pretreatment, the steady-state permeate flux increases by 569.4 and 391.61 l m^{-2} h^{-1}. The difference between these values is not as strong as without pretreatment.

Fig. 12 shows that dispersion with pretreatment has a smaller tendency to reach a limiting flux compared to that without pretreatment. The pretreated dispersion curve is more linear than the curve for dispersion without pretreatment. This is probably caused by lower cake compression and resistance than those obtained without pretreatment.

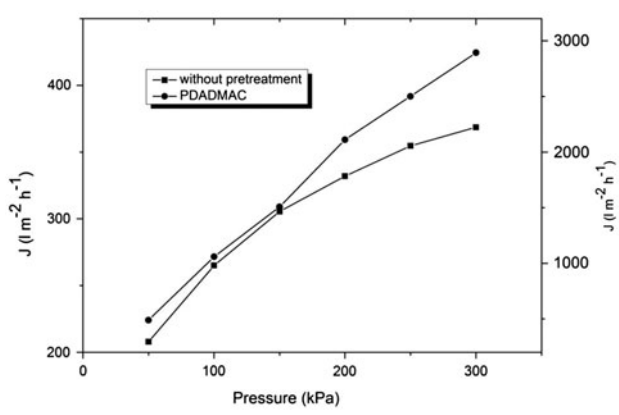

Fig. 12. The dependencies of steady-state permeate flux at transmembrane pressure.

3.6. Validation of the mathematical model

In Fig. 13, we can see the effect of transmembrane pressure on steady-state permeate flux during crossflow microfiltration of dispersion without pretreatment. Comparison of the experimental data points with the values predicted by the mathematical model shows that the model is not able to predict the permeate flux accurately. The curves are similar, but the values obtained from the mathematical model are significantly lower than those obtained experimentally.

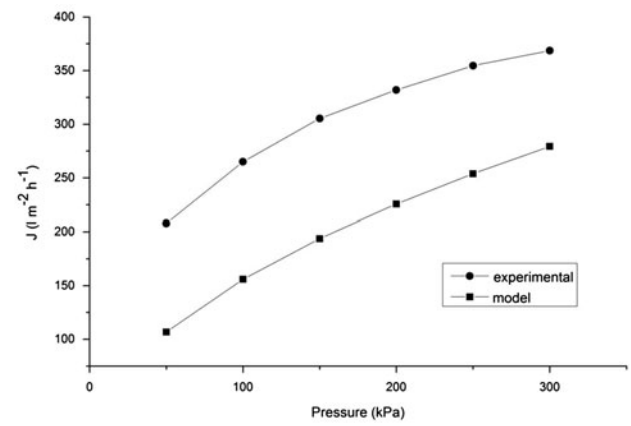

Fig. 13. Effect of transmembrane pressure on steady-state permeate flux during the crossflow microfiltration of model dispersion (without pretreatment).

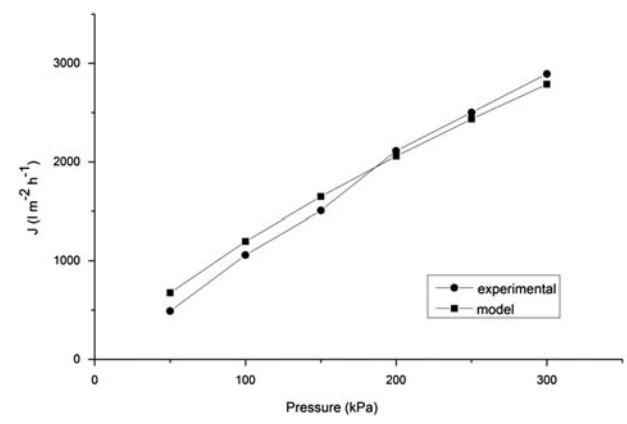

Fig. 14. Effect of transmembrane pressure on steady-state permeate flux during the crossflow microfiltration of model dispersion (pretreatment by 30 mg l^{-1} PDADMAC).

The dependencies of steady-state permeate flux on the transmembrane pressure during crossflow microfiltration with pretreatment by 30 mg l^{-1} PDADMAC are shown in Fig. 14. From this figure, it is clear that the model is able to predict the steady-state permeate flux for crossflow microfiltration with pretreatment quite accurately. This result has a considerable practical importance and may reduce costs compared to physical experiments.

Differences between the model and experiment can be caused by simplifications used in the derivation of the mathematical model. These simplifications are, for example, neglecting the resistance of the boundary layer and neglecting the lateral migration of particles due to inertial lift or the flowing cake. The mathematical model also neglects the effect of the ζ-potential of the particles and membrane.

4. Conclusions

The results of the experiments presented in the previous sections have shown that during crossflow membrane microfiltration of titanium dioxide dispersion, the values of steady-state permeate flux and the particle size distribution were significantly affected by the choice of the respective coagulant, with PDADMAC, PAM, and PACA being of interest in this study. The use of coagulants could significantly decrease the membrane fouling, thus increasing the resultant permeate flux. The most suitable coagulant for the crossflow microfiltration of titanium dioxide was PDADMAC and its optimal dosage was 30 mg l^{-1}. Pretreatment of the feed by 30 mg l^{-1} PDADMAC led to a permeate flux that was more than three times higher than that obtained without any pretreatment. The largest average particle size of the dispersion was 8.65 μm and was obtained at the optimum concentration of 30 mg l^{-1} PDADMAC. This average particle size was 18 times higher than the average particle size of dispersion without pretreatment. The other two coagulants tested did not lead to improvements as large as those given by PDADMAC; the optimal dosage of PAM was 100 mg l^{-1} but feed pretreatment with this PAM dosage led to a permeate flux that was only 10% higher than obtained in experiments without pretreatment. This is a considerably lower permeate flux than that obtained with pretreatment by PDADMAC. Regarding PACA, no optimal dosage was found because, for each dosage, pretreatment of the feed by PACA always led to a lower permeate flux compared to that obtained without pretreatment.

The results of the experiments showed that coagulation could decrease the membrane fouling and increase the permeate flux. On the other hand, in some cases, coagulation could also decrease the permeate flux. Finally, although the average particle size was mostly increased by coagulation, in some cases it was smaller than that of unpretreated dispersion material. Based on the experiments performed, it can be concluded that the proper coagulant has to be carefully selected because its type and the actual dosage both have important impacts on the resultant permeate flux.

The results of the experiments presented in the previous sections show that the mathematical model is able to predict the steady-state permeate flux quite accurately in the case with pretreatment. This model can be considered as a first approximation to explain the physical phenomena involved. Differences between model and experiment can be caused by simplifications used in the derivation of the mathematical model. These simplifications are, for example, neglecting the resistance of the boundary layer and neglecting lateral migration of particles due to inertial lift or the flowing cake. The mathematical model also neglects the effect of the ζ-potential of the particles and membrane.

However, it needs further verifications with more microfiltration data for a detailed understanding of the coagulation process. For future work is suitable improvement of the mathematical model and its verification under various conditions.

Acknowledgements

This work was supported and financed by the University of Pardubice under grant number SGS_2016_002.

List of symbols

J	—	permeate flux (l m^{-2} h^{-1})
k_1	—	particle constant (–)
K	—	membrane permeability (l m^{-2} h^{-1} bar^{-1})
ΔP	—	pressure difference (Pa)
R_c	—	resistance of the filtration cake (m^{-1})
$\hat{R}_c$	—	cake resistance per unit thickness (m^{-1})
R_f	—	resistance caused by pore blocking and adsorption on pore surfaces (m^{-1})
R_m	—	resistance of the membrane (m^{-1})
R_t	—	total resistance to permeate flow (m^{-1})
S	—	filtration cake compressibility constant (–)
U	—	crossflow velocity (m s^{-1})
α_0	—	particle constant (–)
δ_c	—	thickness of the filtration cake (m)
μ	—	dynamic viscosity of suspension (Pa s)
μ_0	—	dynamic viscosity of solvent (Pa s)
ρ_s	—	density of the particles constituting the filtration cake (kg m^{-3})
T	—	time (s)

τ_w — shear stress at membrane wall (Pa)
Φ_b — particle volume fraction of the dispersion (–)
Φ_c — particle volume fraction in the filtration cake (–)

References

[1] H. Strathmann, L. Giorno, E. Drioli, Introduction to Membrane Science and Technology, Wiley, Weinheim, 2011.
[2] M. Mulder, Basic Principles of Membrane Technology, second ed., Kluwer Academic Publishers, Dordrecht, 1996.
[3] L.K. Wang, J.P. Chen, Y. Hung, N.K. Shammas, Membrane and Desalination Technologies, Humana Press, New York, NY, 2011.
[4] P. Mikulášek, P. Doleček, H. Šedá, J. Cakl, Alumina-ceramic microfiltration membranes: Preparation, characterization and some properties, Develop. Chem. Eng. Miner. Process. 2 (1994) 115–123.
[5] P. Mikulášek, Pressure Driven Membrane Processes (in Czech), Vydavatelství VŠCHT Praha, Praha, 2013.
[6] E. Baruth, Water Treatment Plant Design, fourth ed., McGraw-Hill, New York, NY, 2005.
[7] A.K. Pabby, S.S.H. Rizvi, A.M. Sastre, Handbook of Membrane Separations, CRC Press, Boca Raton, 2008.
[8] L. Erdei, C.Y. Chang, S. Vigneswaran, In-line flocculation-submersed MF/UF membrane hybrid system in tertiary wastewater treatment, Sep. Sci. Technol. 43 (2008) 1839–1851.
[9] C. Park, S.W. Hong, T.H. Chung, Y.S. Choi, Performance evaluation of pretreatment processes in integrated membrane system for wastewater reuse, Desalination 250 (2010) 673–676.
[10] H. Zhu, X. Wen, X. Huang, Characterization of membrane fouling in a microfiltration ceramic membrane system treating secondary effluent, Desalination 284 (2012) 324–331.
[11] P. Bhattacharya, S. Dutta, S. Ghosh, Crossflow microfiltration using ceramic membrane for treatment of sulphur black effluent from garment processing industry, Desalination 261 (2010) 67–72.
[12] B. Zhao, D. Wang, T. Li, C.W.K. Chow, C. Huang, Influence of floc structure on coagulation–microfiltration performance: Effect of Al speciation characteristics of PACls, Sep. Purif. Technol. 72 (2010) 22–27.
[13] J. Wang, J. Guan, S.R. Santiwong, T.D. Waite, Characterization of floc size and structure under different monomer and polymer coagulants on microfiltration membrane fouling, J. Membr. Sci. 321 (2008) 132–138.
[14] B. Hofs, D. Vries, W.G. Siegers, E.F. Beerendonk, E.R. Cornelissen, Influence of water type and pretreatment method on fouling and performance of an Al_2O_3 microfiltration membrane, Desalination 299 (2012) 28–34.
[15] S. Wang, C. Liu, Q. Li, Fouling of microfiltration membranes by organic polymer coagulants and flocculants: Controlling factors and mechanisms, Water Res. 45 (2011) 357–365.
[16] B. Wu, Y. An, Y. Li, F.S. Wong, Effect of adsorption/coagulation on membrane fouling in microfiltration process post-treating anaerobic digestion effluent, Desalination 242 (2009) 183–192.
[17] C.M. Silva, D.W. Reeve, H. Husain, H.R. Rabie, K.A. Woodhouse, Model for flux prediction in high-shear microfiltration systems, J. Membr. Sci. 173 (2000) 87–98.
[18] M.C. Porter, What, when, and why of membranes—MF, UF, RO, AIChE Symp. Ser. 73 (1977) 83–103.
[19] Y. Zhou, G.V. Franks, Flocculation mechanism induced by cationic polymers investigated by light scattering, Langmuir 22 (2006) 6775–6786.
[20] A. Blanco, E. Fuente, C. Negro, J. Tijero, Flocculation monitoring: Focused beam reflectance measurement as a measurement tool, Can. J. Chem. Eng. 80 (2002) 734–740.
[21] P. Bacchin, A possible link between critical and limiting flux for colloidal systems: Consideration of critical deposit formation along a membrane, J. Membr. Sci. 228 (2004) 237–241.